Nanoscale Flexible Low-Voltage Organic Thin-Film Transistors

Hagen Klauk

email: H.Klauk@fkf.mpg.de
Max Planck Institute for Solid State Research, Heisenbergstr. 1, 70569 Stuttgart, Germany
Keywords: organic thin-film transistors, high-frequency thin-film transistors, nanoscale transistors

ABSTRACT

Organic thin-film transistors with channel lengths and gate-to-contact overlaps as small as 100 nm have been fabricated on polymeric substrates using electron-beam lithography. The transistors have on/off current ratios up to 10^{10}, subthreshold swings as small as 70 mV/decade, and signal delays as small as 14 ns at a supply voltage of 3 V.

1 Introduction

Thin-film transistors (TFTs) based on conjugated organic semiconductors can typically be fabricated at relatively low process temperatures, usually around or below 100 °C, and thus not only on glass, but also on polymeric substrates. This makes organic TFTs potentially useful for flexible electronics applications, such as rollable active-matrix displays and bendable integrated circuits.

The dynamic TFT performance is determined mainly by their critical dimensions, i.e., by the channel length and the parasitic gate-to-source and gate-to-drain overlaps. How small these can be made depends to a large extent on the patterning process. The resolution limit of most of the lithography techniques typically utilized for organic-TFT fabrication, including laser lithography [1,2], photolithography [3,4] and stencil lithography [5,6], is approximately 1 µm. Organic TFTs fabricated using these techniques have voltage-normalized transit frequencies up to 7 MHz/V (21 MHz at a gate-source voltage of 3 V [5]). For comparison, vertical organic permeable-base transistors in which the distance traveled by the charge carriers from the emitter to the collector is defined by a deposited-layer thickness and only the parasitic overlaps are defined by lithography, have demonstrated voltage-normalized frequencies up to 25 MHz/V [7].

Electron-beam lithography is a high-resolution patterning technique that makes it possible to fabricate organic TFTs with lateral dimensions as small as about 100 nm on polymeric substrates [8]. Here, we report on the static and dynamic characteristics of p-channel and n-channel organic TFTs with channel lengths and gate-to-contact overlaps as small as 100 nm fabricated by electron-beam lithography on flexible polyethylene naphthalate (PEN) substrates. The TFTs have on/off current ratios as large as 10^{10} and subthreshold swings as small as 70 mV/decade. Unipolar inverters display characteristic switching-delay time constants as small as 14 ns at a supply voltage of 3 V, corresponding to a voltage-normalized frequency of 12 MHz/V.

2 Experiment

The TFTs were fabricated in the inverted coplanar (bottom-gate, bottom-contact) device architecture on 125-µm-thick flexible polyethylene naphthalate (Teonex Q65 PEN) substrates. Figure 1 shows a schematic cross section of the TFTs.

The aluminum gate electrodes and gold source/drain contacts were deposited by thermal evaporation in vacuum and patterned by electron-beam lithography and lift-off, using a two-layer poly(methyl methacrylate) (PMMA) resist and a Raith eLINE electron-beam lithography system with an electron-beam voltage of 20 kV and an exposure dose of 370 µC/cm^2.

The surface of the aluminum gate electrodes was briefly exposed to oxygen plasma to produce an aluminum oxide (AlO_x) gate dielectric with a thickness of about 6 nm [9]. To promote a favorable morphology of the organic semiconductor in the channel region of the TFTs and on the surface of the gold source/drain contacts, the substrate was immersed first into an alkyl- or fluoroalkylphosphonic acid solution, allowing the formation of a hydrophobic self-assembled monolayer (SAM) with a thickness of about 2 nm on the surface of the aluminum oxide gate dielectric [10], followed by immersion into a solution of a thiol or mercaptan to functionalize the surface of the gold source and drain contacts with a chemisorbed monolayer, with the intent of minimizing the contact resistance of the TFTs [5,11].

In the last process step, the semiconductor was deposited by thermal sublimation in vacuum through a manually aligned stencil mask [6]. The semiconductors diphenyl-dinaphtho-[2,3-b:2',3'-f]thieno[3,2-b]thiophene (DPh-DNTT) [12] and ActivInk N1100 [13] were chosen for the p-channel and the n-channel TFTs, respectively.

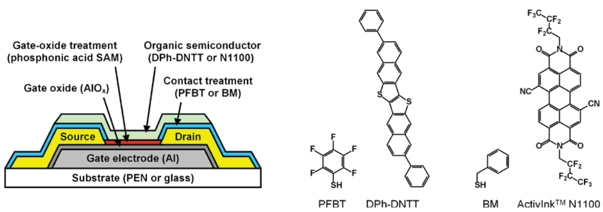

Fig. 1. Schematic TFT cross section and structures of the organic semiconductors (DPh-DNTT, N1100) and of the molecules for the functionalization of the source and drain contacts.

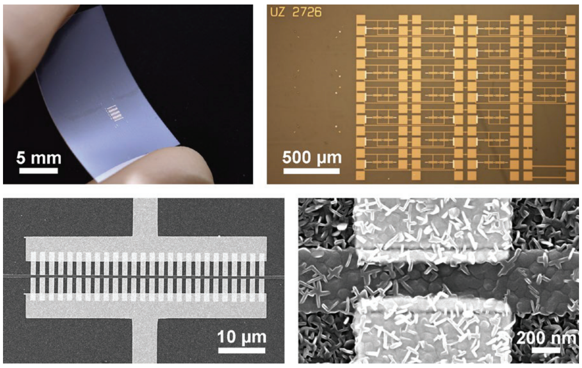

Fig. 2. Photographs and scanning electron microscopy (SEM) images of TFTs fabricated by electron-beam lithography on a flexible PEN substrate.

3 Results

Using electron-beam lithography, we have fabricated organic TFTs with channel lengths and gate-to-contact overlaps as small as 100 nm on polymeric substrates. The air-stable small-molecule organic semiconductors DPh-DNTT [12] and ActivInk N1100 [13] were selected for the p-channel and n-channel TFTs, respectively. The capabilities of direct-write electron-beam lithography for the fabrication of dense arrays of nanoscale organic TFTs with excellent accuracy on flexible substrates is illustrated in Figure 2.

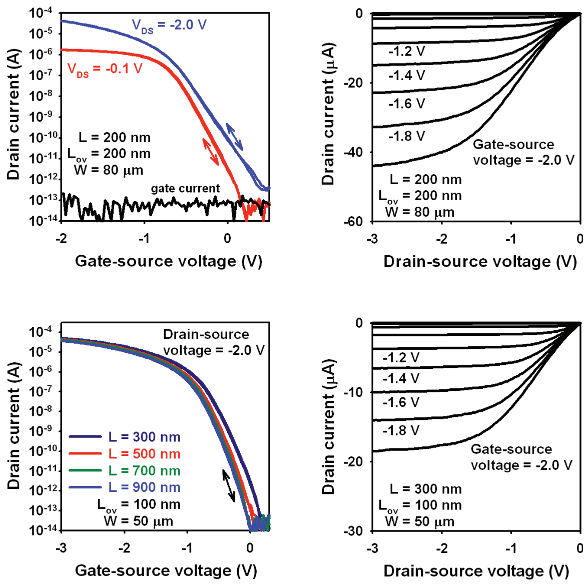

Fig. 3. Top: Transfer and output characteristics of a p-channel DPh-DNTT TFT with a channel length of 200 nm and gate-to-contact overlaps of 200 nm. Bottom: Transfer characteristics of DPh-DNTT TFTs with channel lengths of 300, 500, 700, and 900 nm and gate-to-contact overlaps of 100 nm, and output characteristics of the DPh-DNTT TFT with a channel length of 300 nm.

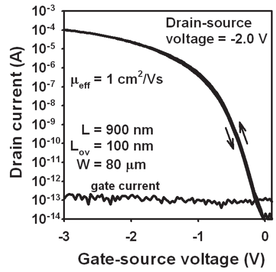

Fig. 4. Transfer characteristics of a p-channel DPh-DNTT TFT with a channel length of 900 nm and gate-to-contact overlaps of 100 nm, showing an on/off current ratio of 10^{10}, the largest on/off ratio reported to date for flexible organic TFTs.

The measured current-voltage characteristics of p-channel DPh-DNTT TFTs with channel lengths ranging from 200 to 900 nm, gate-to-contact overlaps of 100 or 200 nm, and a channel width of 50 or 80 µm are shown in Figure 3. The transfer characteristics indicate on/off current ratios between 1×10^8 and 4×10^9, subthreshold swings between 80 and 150 mV/decade, turn-on voltages between 0.0 and 0.4 V, and effective charge-carrier mobilities between 0.1 and 0.4 cm^2/Vs. For a channel length of 900 nm, gate-to-contact overlaps of 100 nm, and a channel width of 80 µm, the on/off current ratio reaches 10^{10} (Figure 4). This is the largest on/off current ratio reported to date for flexible organic TFTs.

For mobile or wearable electronics systems, low-voltage device and circuit operation is of critical importance. Figure 5 summarizes the transfer and output characteristics of a p-channel DPh-DNTT TFT with a channel length of 600 nm, gate-to-contact overlaps of 400 nm, and a channel width of 80 µm measured with a maximum gate-source voltage of -1 V. The transfer characteristics indicate a turn-on voltage of 0.0 V, a subthreshold swing of 70 mV/decade, and an on/off current ratio of 3×10^8; this is the largest on/off current ratio reported to date for organic TFTs over a gate-source voltage range from 0 to ±1 V or less [14].

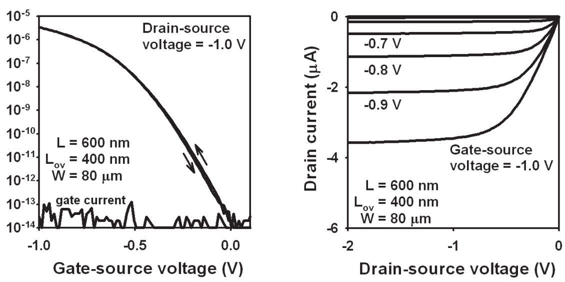

Fig. 5. Low-voltage operation of a p-channel DPh-DNTT TFT having a channel length of 600 nm and gate-to-contact overlaps of 400 nm.

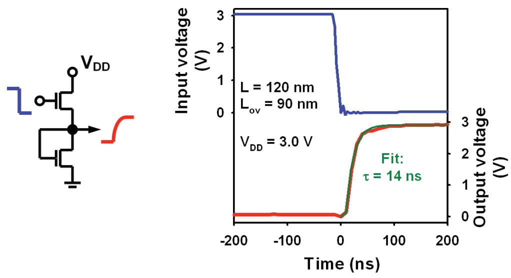

Fig. 6. Circuit schematic and dynamic characteristics of a unipolar zero-V_{GS} inverter based on two p-channel DPh-DNTT TFTs with channel lengths of 120 nm and gate-to-contact overlaps of 90 nm. The output signal indicates a signal-delay time constant of 14 ns at a supply voltage of 3 V.

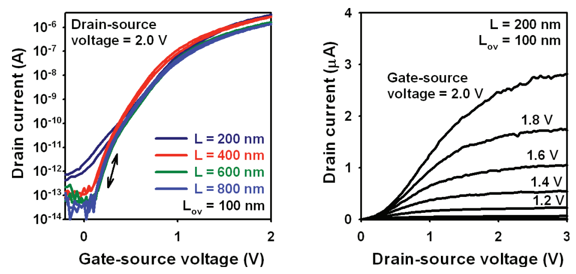

Fig. 7. Measured transfer characteristics of n-channel N1100 TFTs with channel lengths of 200, 400, 600 and 800 nm, gate-to-contact overlaps of 100 nm, and a channel width of 50 µm, and output characteristics of the TFT with a channel length of 200 nm.

To evaluate the dynamic performance of the nanoscale p-channel TFTs, we fabricated unipolar inverters designed in a zero-V_{GS} circuit topology [15]. These inverters are based on two p-channel DPh-DNTT TFTs which both have a channel length of 120 nm and gate-to-contact overlaps of 90 nm. Figure 6 shows the circuit schematic and the measured dynamic characteristics of such an inverter. From the inverter's dynamic characteristics, which were measured by applying a square-wave voltage with an amplitude of 3 V to the input of the inverter while recording the output response using a high-impedance probe and an oscilloscope, a characteristic switching-delay time constant (τ) of 14 ns is extracted for a supply voltage of 3 V. This corresponds to an equivalent frequency [$f_{eq} = 1/(2\cdot\tau)$] of 36 MHz.

In addition to p-channel TFTs (based on DPh-DNTT as the semiconductor), we also fabricated n-channel organic TFTs, using Polyera ActivInk N1100 as the semiconductor [13]. The measured current-voltage characteristics of n-channel N1100 TFTs with channel lengths ranging from 200 to 800 nm and gate-to-contact overlaps of 150 nm fabricated on a glass substrate are summarized in Figure 7. The transfer characteristics indicate on/off current ratios up to 10^8, subthreshold swings as small as 80 mV/decade, and turn-on voltages between 0.1 and -0.5 V. This is the best static performance reported to date for nanoscale n-channel organic TFTs.

4 Discussion

The nanoscale TFTs and inverters reported here were fabricated using electron-beam lithography. While the main drawback of electron-beam lithography is its low throughput, this does not preclude the potential of using electron-beam lithography to fabricate organic TFTs and circuits on a larger scale. Just like the throughput of other maskless patterning techniques, such as laser lithography [1,2] and inkjet printing [16], can be greatly enhanced by the implementation of multiple beams or multiple nozzles [17], the efficiency of electron-beam lithography can be massively increased as well by implementing arrays of individually addressable electron beams [18,19]. These considerations notwithstanding the primary purpose of the work reported here was not to suggest electron-beam lithography as a method for the mass production of organic TFTs, but rather to confirm that organic TFTs with channel lengths and gate-to-contact overlaps in the range of a few hundred nanometers fabricated on flexible plastic substrates can provide useful static performance, including near-zero turn-on voltages as well as off-state drain currents, on/off current ratios, and subthreshold swings comparable to the best values reported for long-channel organic TFTs.

5 Conclusions

In summary, we have used direct-write electron-beam lithography to fabricate p-channel and n-channel organic TFTs with channel lengths as small as 120 nm and gate-to-contact overlaps as small as 90 nm on flexible polymeric substrates. The TFTs have on/off current ratios as large as 10^{10} and subthreshold swings as small as 70 mV/decade. Unipolar inverters display a characteristic switching-delay time constant of 14 ns at a supply voltage of 3 V, corresponding to a supply voltage-normalized equivalent frequency of about 12 MHz/V. Better dynamic performance can be expected by reductions of the contact resistance; for example, for a contact resistance of 10 Ωcm (the smallest contact resistance reported for organic TFTs [5]), a transit frequency above 100 MHz at 3 V can be expected.

Acknowledgements

The authors would like to thank Kazuo Takimiya (RIKEN Center for Emergent Matter Science, Wako, Saitama, Japan) and Koichi Ikeda, Yuichi Sadamitsu, and Satoru Inoue (Nippon Kayaku, Tokyo, Japan) for providing DPh-DNTT. This work was partially funded by the German Research Foundation (DFG) under grants KL 2223/6-2 (SPP FFlexCom), KL 2223/7-1 and INST 35/1429-1 (SFB 1249).

References

[1] A. Perinot, M. Giorgio, V. Mattoli, D. Natali, and M. Caironi, “Organic Electronics Picks Up the Pace: Mask-Less, Solution Processed Organic Transistors Operating at 160 MHz,” Adv. Sci., Vol. 8, p. 2001098 (2021).

[2] B. Passarella, A. D. Scaccabarozzi, M. Giorgio, A. Perinot, S. M. Barbier, J. Martin, and M. Caironi, “Direct-writing of organic field-effect transistors on plastic achieving 22 MHz transition frequency,” Flex. Print. Electronics, Vol. 5, p. 034001 (2020).

[3] T. Sawada, A. Yamamura, M. Sasaki, K. Takahira, T. Okamoto, S. Watanabe, and J. Takeya, “Correlation between the static and dynamic responses of organic single-crystal field-effect transistors,” Nature Commun., Vol. 11, p. 4839 (2020).

[4] M. Kitamura and Y. Arakawa, “High current-gain cutoff frequencies above 10 MHz in n-channel C_{60} and p-channel pentacene thin-film transistors,” Jpn. J. Appl. Phys., Vol. 50, p. 01BC01 (2011).

[5] J. W. Borchert, U. Zschieschang, F. Letzkus, M. Giorgio, R. T. Weitz, M. Caironi, J. N. Burghartz, S. Ludwigs, and H. Klauk, “Flexible low-voltage high-frequency organic thin-film transistors,” Sci. Adv., Vol. 6, p. eaaz5156 (2020).

[6] T. Zaki, R. Rödel, F. Letzkus, H. Richter, U. Zschieschang, H. Klauk, and J. N. Burghartz, “S-parameter characterization of submicrometer low-voltage organic thin-film transistors,” IEEE Electron Device Lett., Vol. 34, p. 520 (2013).

[7] E. Guo, S. Xing, F. Dollinger, R. Hübner, S.-J. Wang, Z. Wu, K. Leo, and H. Kleemann, “Integrated complementary inverters and ring oscillators based on vertical-channel dual-base organic thin-film transistors,” Nature Electronics, Vol. 4, p. 588 (2021).

[8] U. Zschieschang, U. Waizmann, J. Weis, J. W. Borchert, and H. Klauk, “Nanoscale flexible organic thin-film transistors,” Sci. Adv., Vol. 8, p. e abm9845 (2022).

[9] M. Geiger, M. Hagel, T. Reindl, J. Weis, R. T. Weitz, H. Solodenko, G. Schmitz, U. Zschieschang, H. Klauk, and R. Acharya, “Optimizing the plasma oxidation of aluminum gate electrodes for ultrathin gate oxides in organic transistors,” Sci. Rep., Vol. 11, p. 6382 (2021).

[10] R. Acharya, B. Peng, P. K. L. Chan, G. Schmitz, and H. Klauk, “Achieving Ultralow Turn-On Voltages in Organic Thin-Film Transistors: Investigating Fluoroalkylphosphonic Acid Self-Assembled Monolayer Hybrid Dielectrics,” ACS Appl. Mater. Interfaces, Vol. 11, p. 27104 (2019).

[11] J. W. Borchert, R. T. Weitz, S. Ludwigs, and H. Klauk, “A Critical Outlook for the Pursuit of Lower Contact Resistance in Organic Transistors,” Adv. Mater., Vol. 34, p. 2104075 (2022).

[12] K. Niimi, M. J. Kang, E. Miyazaki, I. Osaka, and K. Takimiya, “General synthesis of dinaphtho[2,3-b:2’,3’-f]thieno[3,2-b]thiophene (DNTT) derivatives,” Org. Lett., Vol. 13, p. 3430 (2011).

[13] B. A. Jones, M. J. Ahrens, M.-H. Yoon, A. Facchetti, T. J. Marks, and M. R. Wasielewski, “High-mobility air-stable n-type semiconductors with processing versatility: Dicyanoperylene-3,4:9,10-bis(dicarboximides),” Angew. Chem. Int. Ed., Vol. 43, p. 6363 (2004).

[14] U. Zschieschang, V. P. Bader, and H. Klauk, “Below-one-volt organic thin-film transistors with large on/off current ratios,” Org. Electronics, Vol. 49, p. 179 (2017).

[15] M. Geiger, R. Lingstädt, T. Wollandt, J. Deuschle, U. Zschieschang, F. Letzkus, J. N. Burghartz, P. A. van Aken, R. T. Weitz, and H. Klauk, “Subthreshold swing of 59 mV decade^{-1} in nanoscale flexible ultralow-voltage organic transistors,” Adv. Electron. Mater., Vol. 8, p. 2101215 (2022).

[16] J. Kwon, H. Matsui, W. Kim, S. Tokito, and S. Jung, “Static and dynamic response comparison of printed, single- and dual-gate 3-D complementary organic TFT inverters,” IEEE Electr. Dev. Lett., Vol. 40, p. 1277 (2019).

[17] A. Khan, K. Rahman, S. Ali, S. Khan, B. Wang, and A. Bermak, “Fabrication of circuits by multi-nozzle electrohydrodynamic inkjet printing for soft wearable electronics,” J. Mater. Res., Vol. 36, p. 3568 (2021).

[18] H. Matsumoto, H. Inoue, H. Yamashita, T. Tamura, and K. Ohtoshi, “Multibeam mask writer MBM-1000,” J. Micro Nanolithogr. MEMS MOEMS, Vol. 17, p. 031205 (2018).

[19] M. Esashi, A. Kojima, N. Ikegami, H. Miyaguchi, and N. Koshida, “Development of massively parallel electron beam direct write lithography using active-matrix nanocrystallinesilicon electron emitter arrays,” Microsyst. Nanoeng., Vol. 1, p. 15029 (2015).